Physica A 392 (2013) 1586–1592

Contents lists available at SciVerse ScienceDirect

Physica A

journal homepage: www.elsevier.com/locate/physa

# Saddle points and rare collisions under scaling approach in a Fermi accelerator with two nonlinear terms

Juliano A. de Oliveira [a,*], Edson D. Leonel [a,b]

[a] Departamento de Física, UNESP - Univ Estadual Paulista, Av.24A, 1515 - 13506-900, Rio Claro, SP, Brazil

[b] Abdus Salam ICTP, 34100 Trieste, Italy

ARTICLE INFO

*Article history:*
Received 11 December 2012
Available online 20 December 2012

*Keywords:*
Fermi accelerator
Rare collisions
Saddle fixed points

ABSTRACT

Rare collisions of a classical particle bouncing between two walls are studied. The dynamics is described by a two-dimensional, nonlinear and area-preserving mapping in the variables velocity and time at the instant that the particle collides with the moving wall. The phase space is of mixed type preventing diffusion of the particle to high energy. Successive and therefore rare collisions are shown to have a histogram of frequency which is scaling invariant with respect to the control parameters. The saddle fixed points are studied and shown to be scaling invariant with respect to the control parameters too.



## 1. Introduction

The traditional one-dimensional Fermi accelerator model consists of a classical particle of mass $M$ which is confined to move between two rigid walls. One is fixed and works only as a returning mechanism for the particle to collides with the other one which is assumed to move in time. This simple system emerged as an attempt of Ulam [1] to model the original idea of Fermi [2] to describe the high energy measured from the cosmic rays. Indeed Fermi claimed that the energy of the cosmic particles could be gained from interactions of the particles with moving magnetic fields existent in the space. Therefore in Ulam's interpretation, the moving wall would indeed represent a moving magnetic field while the particle denotes a cosmic ray. The problem was that after the particle collides with moving wall and leaving the collision zone it moves with constant velocity to infinite. Ulam then imposed the existence of a fixed wall that the particle has to collide and returns for a further collision with the moving wall. The model as proposed failed to explain the cosmic rays high energy. The failure was due to the fact that the dynamics of the particle at high energy exhibits a short time elapsed between collisions leading to a strong correlation of them. The phase space which appears from the model is of mixed type showing both the existence of periodic islands (denoting regular/periodic motion) surrounded by a chaotic sea which is confined by a set of invariant KAM curves of quasi-periodic dynamics. Such a set of curves appear due to the high correlation between the collisions and they work as barriers that do not allow the particle to pass through, therefore setting an upper limit for the velocity growth.

The Fermi–Ulam model was considered after that in many different approaches, using different techniques and as motivation for several experiments [3–15]. The unlimited energy growth, the aim of the Fermi's idea would indeed be implemented if the returning mechanism of the particle for a next collision is changed. Pustylnikov [16] proposed replacing the fixed wall, which leads to correlation in the regime of high energy, to a gravitation field. Indeed, as soon as the particle accumulate energy from the collisions with the moving wall, the interval of time between collisions rises therefore leading to a lose of correlation between two collisions. For certain ranges of control parameters, the invariant KAM curves present in the phase space of the Fermi–Ulam are not observed in the Pustylnikov model. Depending on the combination of control

* Corresponding author. Tel.: +55 1935341511; fax: +55 1935341511.
*E-mail addresses:* julianoantonio@gmail.com (J.A. de Oliveira), edleonel@rc.unesp.br (E.D. Leonel).

0378-4371/$ – see front matter © 2012 Elsevier B.V. All rights reserved.
doi:10.1016/j.physa.2012.12.012

parameters and initial conditions, the particle would exhibit diffusion in the velocity, leading to a phenomenon called as Fermi acceleration. However, either inelastic collision [17] and drag force [18] are shown to be sufficient conditions to suppress the unlimited growth of velocity therefore giving support to the assumption that Fermi acceleration is not a robust phenomenon [19]. It was shown in the literature that the introduction of drag force in the Fermi–Ulam model makes the particle loses energy (velocity) as it passed through a fluid such as a gas [20]. Depending on the initial conditions and control parameters, attractors were observed in the system including sinks and the behaviour around them were discussed.

In this paper we revisit the Fermi–Ulam accelerator model considering that the motion of the moving wall is given by a system of the type crank drive [21]. Our main goal is to understand and describe a specific type of rare collisions, namely as successive collisions, and the behaviour of the velocity of the saddle fixed points in the phase space. To do so, we use a scaling formalism. The dynamics of the model is described by a two-dimensional, nonlinear and area preserving mapping. The phase space is of mixed type and invariant KAM curves limit the energy gain of the bouncing particle. However in the limit of the radii of the crank approaching the length of the connecting rod, the movement of the moving wall becomes very fast for certain ranges of phase and very slow for others. In the limit case it may also lead to discontinuities in velocity of the moving wall therefore causing the particle to exhibit unlimited energy growth. However we will not consider such a range here.

The organisation of the paper is as follows. In Section 2 we present the model and discuss the variables and control parameters used. Our discussions regarding the rare events of the successive collisions are also described here together with the scaling for the saddle fixed points. Our conclusions and final remarks are presented in Section 3.

## 2. The model, numerical results and scaling formalism

In this section we revisited the model discussed in Ref. [21] aiming to understand and describe a set of rare collisions that the model exhibits, namely the successive collisions. Indeed the model describes the dynamics of a classical particle of mass $M$ bouncing between two rigid walls. One of then is fixed at $x = \ell$ and the motion of the other wall is given by an equation of the type $s(t) = R\cos(\omega t) + \sqrt{L^2 - R^2\sin^2(\omega t)}$, where $\omega$ is the frequency of oscillation, $R$ denotes the radii of the crank, $L$ the length of the connecting rod. To define the initial conditions we consider that at the time $t = t_n$, the particle is at the position $x_p(t_n) = s(t_n)$ with velocity $v = v_n > 0$. Given the initial conditions, the dynamics may present two different kinds of collisions, such as: (i) a single hit with the moving wall or; (ii) multiple collisions with the moving wall. In the second case, the particle suffers a collision with the moving wall but, before it leaves the collision zone, which is defined as $x \in [-R, R]$, the particle has successive impacts with the moving wall. These impacts are rare in the dynamics and happen at the limit of low velocity. The probability of observing one successive collision is larger than observing two, that is larger than observing three and so on.

To write the mapping that describes the dynamics it is convenient to define dimensionless variables. We define $\epsilon = R/\ell$, $r = R/L$, $V_n = v_n/(\omega\ell)$ and measure the time in terms of the number of oscillations of the moving wall $\phi_n = \omega t_n$. We consider that the range for $\epsilon$ is $\epsilon \in [0, 1]$ and for $r$ is $r \in [0, 1]$. The limit of $r \to 0$ corresponds to $L \to \infty$ and $r \to 1$ is obtained for $L \to R^+$. Using the new variables, we write the mapping as

$$T : \begin{cases} \phi_{n+1} = [\phi_n + \Delta T_n] \bmod (2\pi) \\ V_{n+1} = V_n^* - 2\epsilon\sin(\phi_{n+1})\left(1 + \dfrac{r\cos(\phi_{n+1})}{\sqrt{1 - r^2\sin^2(\phi_{n+1})}}\right), \end{cases} \tag{1}$$

where $V_n$ and $\Delta T_n$ depend on the kind of collision. For the case where the particle leaves the collision zone, $V_n^* = V_n$ and $\Delta T_n = \phi_T + \phi_c$, where $\phi_T$ corresponds to the elapsed time the particle spends travelling from the last collision with the moving wall, up to suffering an elastic reflection with the fixed wall and being reflected backwards, therefore until the entrance of the moving wall. Thus, $\phi_T$ is given by

$$\phi_T = \frac{2 + \left(\frac{\epsilon}{r} - \frac{\epsilon}{r}\sqrt{1 - r^2\sin^2(\phi_n)}\right) - \epsilon\cos(\phi_n) - \epsilon}{V_n}. \tag{2}$$

The term $\phi_c$ is numerically obtained from $F(\phi_c) = 0$ for $\phi_c \in [0, 2\pi)$, where the function $F(\phi_c)$ is given by

$$F(\phi_c) = \epsilon\cos(\phi_n + \phi_T + \phi_c) + \frac{\epsilon}{r}\sqrt{1 - r^2\sin^2(\phi_n + \phi_T + \phi_c)} - \frac{\epsilon}{r} - \epsilon + V_n\phi_c. \tag{3}$$

For the case of multiple collisions with the moving wall, $V_n^* = -V_n$ and $\Delta T_n = \phi_c$ with $\phi_c$ obtained by the solutions of $G(\phi_c) = 0$ with $G(\phi_c)$ given by

$$G(\phi_c) = \epsilon\cos(\phi_n + \phi_c) - \epsilon\cos(\phi_n) - V_n\phi_c + \frac{\epsilon}{r}\sqrt{1 - r^2\sin^2(\phi_n + \phi_c)} - \frac{\epsilon}{r}\sqrt{1 - r^2\sin^2(\phi_n)}. \tag{4}$$

A solution of the function $G(\phi_c)$ for $\phi_c \in (0, 2\pi]$ is obtained numerically considering an accuracy of $10^{-12}$ and corresponds to a collision of the particle with the moving wall.

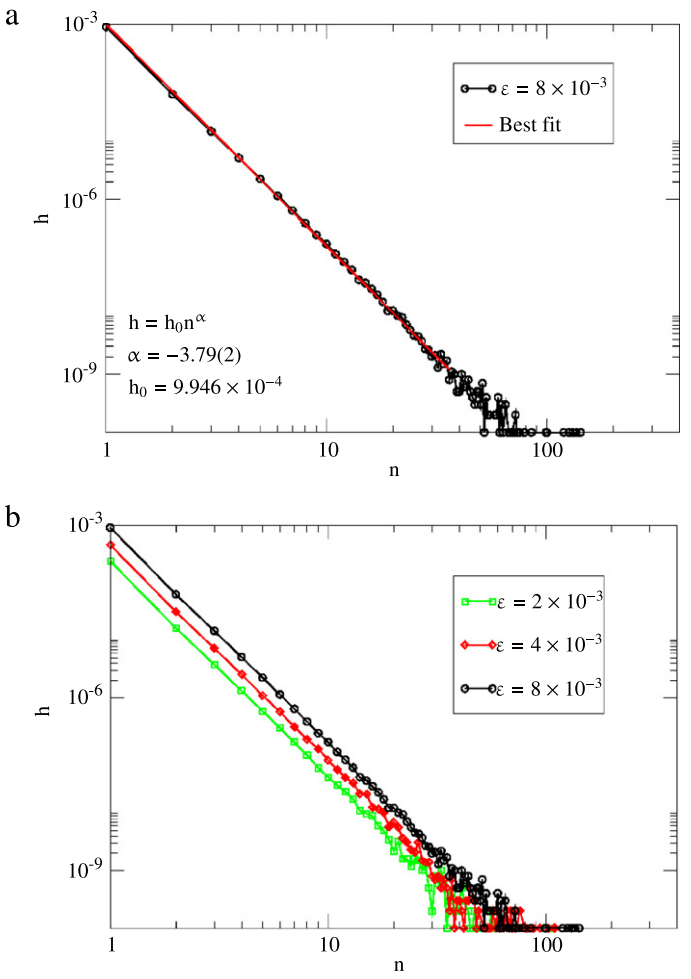


**Fig. 1.** (Colour online) Histogram of successive collisions of the particle with the moving wall. The control parameters used were $r = 0.01$, and: (a) $\epsilon = 8 \times 10^{-3}$ and (b) different values of $\epsilon$ (as labelled in the figure). $n$ corresponds to the number successive collisions with the moving wall while $h$ denotes its frequency.

Let us now discuss the statistics of the successive collisions. Two conditions are needed for the particle to have a successive collision with the moving wall. After obtaining a solution for $F$, a try to $G$ is given, then: (1) the position of the particle must be in $x_p \in [-\epsilon, \epsilon]$; (2) the velocity of the particle $V_n$ must satisfy $V_n < 2\epsilon \sin(\phi_{n+1}) \left(1 + \frac{r\cos(\phi_{n+1})}{\sqrt{1-r^2\sin^2(\phi_{n+1})}}\right)$. In this case, the probability of observing one successive collision is larger than observing two, that is larger than observing three and so on. The distribution of these multiple collisions is described by a power law as shown in Fig. 1. The control parameters used to construct the figure were $r = 0.01$, and: (a) $\epsilon = 8 \times 10^{-3}$ and (b) different values of $\epsilon$ (as labelled in the figure). $n$ corresponds to the number successive collisions with the moving wall while $h$ denotes its frequency.

When applying a power law fitting of the type $h = h_0 n^{\alpha}$ to the data of Fig. 1(a) we obtain $h_0 = 9.946 \times 10^{-4}$ and the exponent $\alpha = -3.79(2)$ for the control parameters $r = 0.01$ and $\epsilon = 8 \times 10^{-3}$. In Fig. 1(b) we use the control parameters $r = 0.01$ and different values of $\epsilon$ (as labelled in the figure). A power law fitting applied to the data shown in Fig. 1(b) also furnishes the exponent $\alpha \simeq -3.79$. We conclude that, at least for this range of control parameters considered, all curves of $h$ have the same slope of decay. A recent discussion on a periodically corrugated waveguide [22] led to obtaining a similar exponent for the successive reflections of the light with the corrugated mirror.

We see from Fig. 1(b) that a rise in the control parameter $\epsilon$ leads the curve of $h$ to also rise keeping the same slope. If we set up a cutting line at $h_c$, say at $h_c = 10^{-6}$, we obtain that

$$n_c = \left(\frac{h_c}{h_0}\right)^{1/\alpha}, \tag{5}$$

where $n_c$ corresponds to the average number of successive collisions at the position $h_c$ in the histogram. A plot of $n_c$ as a function of the control parameter $\epsilon$ is shown in Fig. 2(a) using $h_c = 10^{-6}$. Applying a power law fitting to the data shown

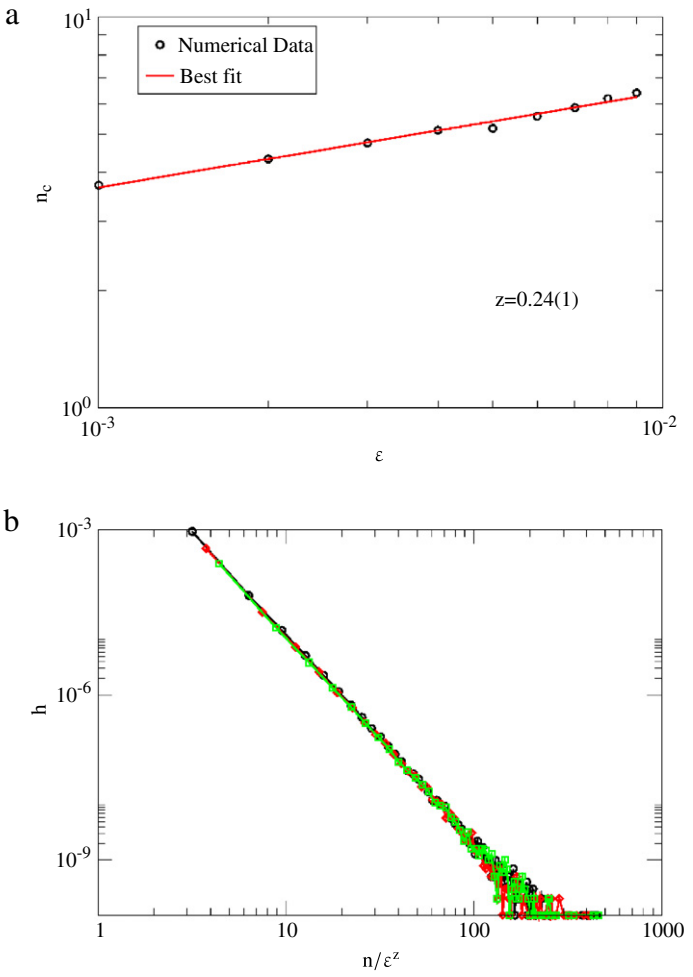


**Fig. 2.** (Colour online) (a) Plot of $n_c$ vs. $\epsilon$ while (b) shows an overlap of the different histograms shown in Fig. 1(b) onto a single and universal plot.

in Fig. 2(a) furnishes the exponent $z = 0.24(1)$. We notice that the exponent $z$ may be obtained as $z \simeq -1/\alpha$. Using the exponent $z$, we can rescale the horizontal axis of Fig. 1(b) and obtain a merger for the three different histograms into a single and universal plot as shown in Fig. 2(b).

Let us now move on and discuss some properties of the phase space. The iteration of the mapping (1) for different initial conditions and considering fixed the parameters $\epsilon = 10^{-3}$ and $r = 0.3$ is shown in Fig. 3. A mixed structure is evident in the sense that a set of periodic islands which are surrounded by a large chaotic sea and KAM curves that limit the unbound growth of the velocity are all observed.

The fixed points of the mapping (1) can be obtained by matching the following conditions: $V_{n+1} = V_n = V$ and $\phi_{n+1} = \phi_n = \phi + 2\pi m$, where $m = 1, 2, 3, \ldots$. We obtained two fixed points, which are: fixed point 1 given by $\left(0, \frac{(1-\epsilon)}{m\pi}\right)$ and fixed point 2 given by $\left(\pi, \frac{(1+\epsilon)}{m\pi}\right)$. We stress that the fixed point 1, is always hyperbolic, while fixed point 2 may be elliptic or hyperbolic, according to the combination of control parameters. If $m > \frac{1+\epsilon}{\pi\sqrt{\epsilon(1-r)}}$ the fixed point 2 is hyperbolic. On the other hand if $0 < m < \frac{1+\epsilon}{\pi\sqrt{\epsilon(1-r)}}$ the fixed point 2 is elliptic. Some of the elliptic fixed points are shown in Fig. 3 as (red) circles while some of the hyperbolic are identified as (blue) squares and (green) diamonds.

We now discuss some properties observed for the saddle fixed point velocity $V$ (fixed point 1) as a function of the parameter $\epsilon$. The behaviour of different saddle velocity curves as a function of $\epsilon$ is shown in Fig. 4 for the control parameter $r = 0.3$ and different values of $m$, as labelled in the figure. We see from Fig. 4(a) that the saddle velocity curves stay almost constant for a relative extent range of the $\epsilon$ until they converge to the null value as the control parameter $\epsilon \to 1$. This fast approach to null values is indeed foreseen by the expression of the velocity of the fixed point 1, i.e., $V = (1-\epsilon)/m\pi$. Based on the behaviour seen in Fig. 4(a) we can suppose that:

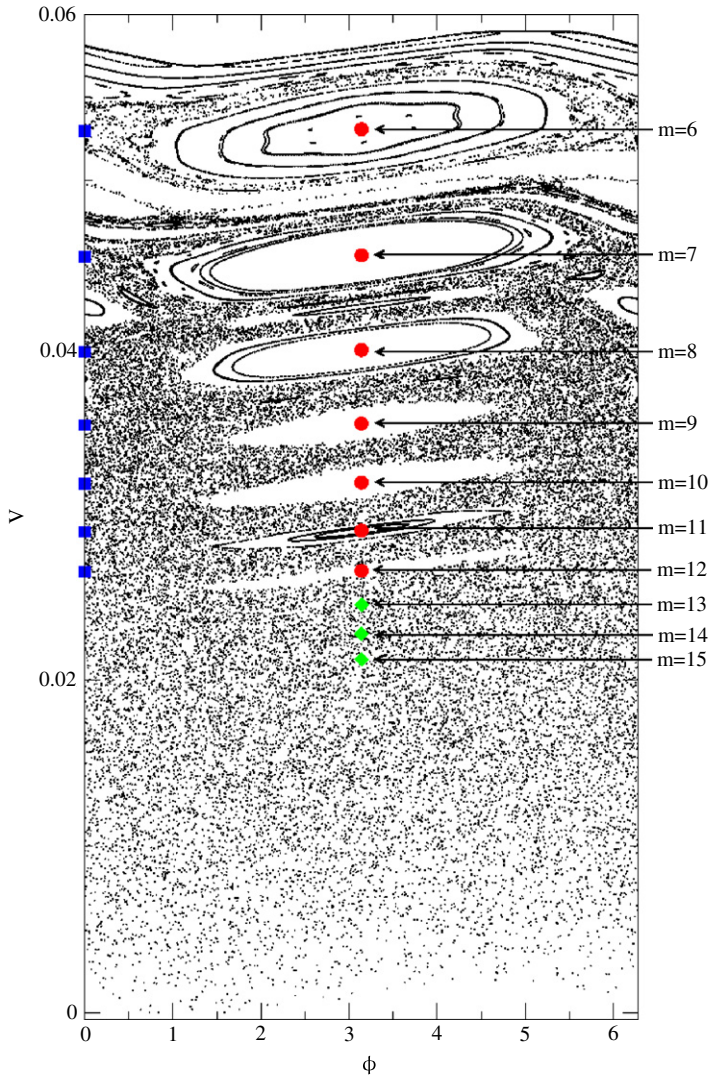


**Fig. 3.** (Colour online) Phase space generated for the mapping (1) for the control parameters $\epsilon = 10^{-3}$ and $r = 0.3$. We used a grid of $10 \times 12$ (one hundred twenty) different initial conditions uniformly distributed in the window $V_0 \in [0.01, 0.057]$ and $\phi_0 \in [0.524, 2\pi]$. Each initial condition was evolved up to $10^3$ iterations.

- (i) The instant of the birth of the fixed point may be described as

$$V_B(\epsilon, m) \propto m^{\sigma}, \tag{6}$$

  where $\sigma$ is an exponent and $m$ is a positive integer number. The index $B$ denotes that the velocity is accounted at the birth of the fixed point, i.e. when the control parameters yield both phase $\phi$ and velocity $V$ being real numbers.

- (ii) Assuming $m$ as fixed, the second scaling hypothesis is

$$V_B(\epsilon) \propto \epsilon^{\mu}, \tag{7}$$

  where $\mu$ is the other exponent.

The exponents $\sigma$ and $\mu$ can be obtained numerically from specific plots. Thus, as an attempt to find them, it is shown in Fig. 5, the corresponding plots of: (a) $V_B$ vs. $\epsilon$ and; (b) $V_B$ vs. $m$ for a fixed parameter $r = 0.3$. A power law fitting to the curves plotted in Fig. 5 furnishes that: (a) $\mu = 0.488(3) \cong 0.5$ and (b) $\sigma = -1.0015(2) \cong -1$. Since the exponents are now known, a merger of four different curves $V$ generated for $r = 0.3$ and different values of control parameters $m$ into the single and universal plot is shown in Fig. 4(b). This result leads us to confirm that the saddle velocity is indeed a scaling invariant.

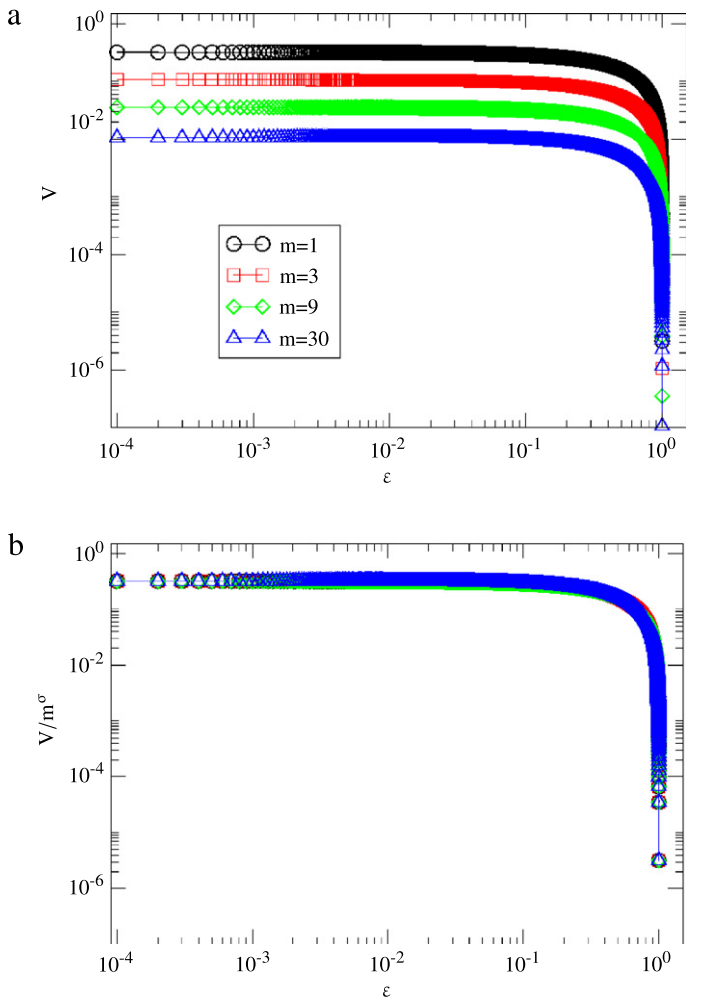


**Fig. 4.** (Colour online) (a) Plot of saddle velocities (fixed point 1) $V$ vs. $\epsilon$ using different values of $m$. (b) Their overlap onto a single and universal plot.

Let us now discuss about the possible effects and consequences of dissipation in the system. The introduction of the dissipation in the system should destroy the mixed structure of the phase space observed for the conservative model. If a small dissipation is introduced in the system, the initial conditions certainly converge into a finite number of periodic attractors, including possible a chaotic one. The number of attractors in the dynamical system depends on the damping coefficient and they exist even for large damping [23,24]. Similar consequences of dissipation observed for the Fermi–Ulam accelerator model may be observed if considering the motion of the moving wall given by a system of the type crank drive. The scaling properties for the successive collisions of the conservative system provided us with the exponent $\alpha = -3.79(2)$. A similar exponent also was observed for the successive reflections of the light with the corrugated mirror in the periodically corrugated waveguide [22]. The scaling properties for the successive collisions may be also be obtained for the dissipative system leading possibly to a different value of the exponent $\alpha$.

## 3. Conclusion

As a short summary, we have studied a conservative version of a classical bouncing ball model under the presence of two nonlinear terms. Our results showed that the successive collisions of the particle with the moving wall are scaling invariant and described by a power law. We used scaling arguments to describe the behaviour of the birth of saddle velocities, which were also shown to be scaling invariants.

## Acknowledgements

JAO thanks CAPES, CNPq and Pró-reitoria de Pesquisa da UNESP. EDL kindly acknowledges the financial support from CNPq, FAPESP and FUNDUNESP, Brazilian agencies.

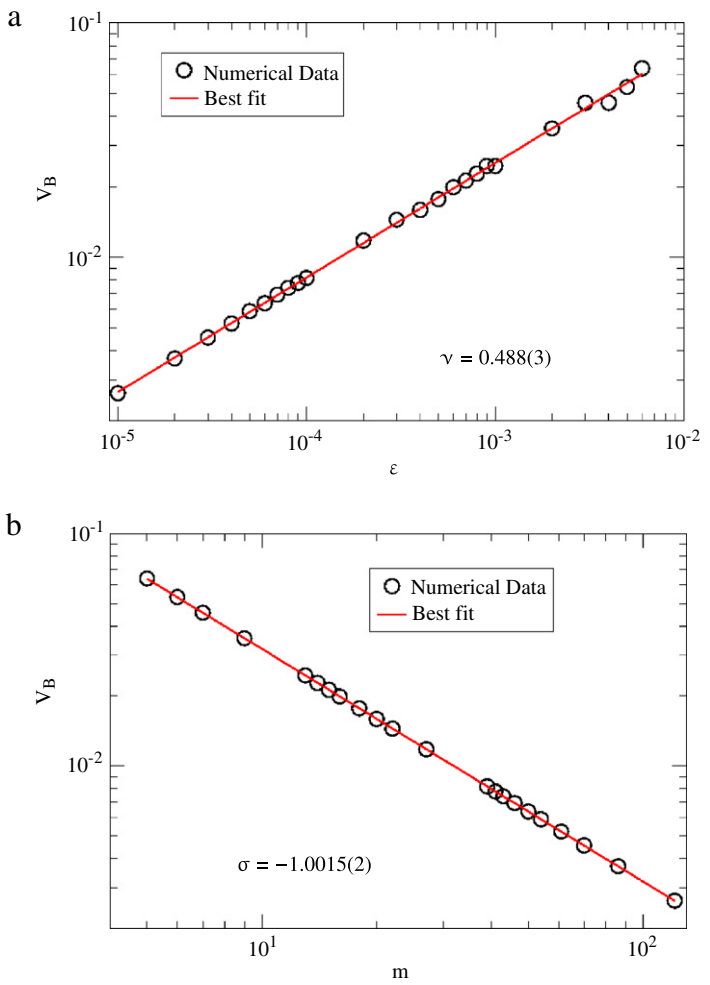


**Fig. 5.** (Colour online) Behaviour of the birth saddle velocities (fixed point 2) as function of: (a) $\epsilon$ and (b) $m$. We consider fixed $r = 0.3$.

## References

[1] S. Ulam, Proceedings of the Fourth Berkeley Symposium on Mathematics, Statistics, and Probability Phenomena, vol. 3, University of California Press, Berkeley, 1961, 315.
[2] E. Fermi, Phys. Rev. 75 (1949) 1169.
[3] K. Szymanski, Y. Labaye, Phys. Rev. E 59 (1999) 2863.
[4] M.A. Malkov, Phys. Rev. E 58 (1998) 4911.
[5] K. Kobayakawa, Y.S. Honda, T. Samura, Phys. Rev. D 66 (2002) 083004.
[6] A. Veltri, V. Carbone, Phys. Rev. Lett. 92 (2004) 143901.
[7] G. Lanzano, et al., Phys. Rev. Lett. 83 (1999) 4518.
[8] A. Steane, P. Szriftgiser, P. Desbiolles, J. Dalibard, Phys. Rev. Lett. 74 (1995) 4972.
[9] G. Michalek, M. Ostrowski, R. Schlickeiser, Sol. Phys. 184 (1999) 339.
[10] A.V. Milovanov, L.M. Zelenyi, Phys. Rev. E 64 (2001) 052101.
[11] M. Franaszek, Z.J. Kowalik, Phys. Rev. A 33 (1986) 3508.
[12] P. Pieranski, J. Malecki, Phys. Rev. A 34 (1986) 582.
[13] Z.J. Kowalik, M. Franaszek, P. Pieranski, Phys. Rev. A 37 (1988) 4016.
[14] G.A. Luna-Acosta, Phys. Rev. A 42 (1990) 7155.
[15] E.D. Leonel, E.P. Marinho, Physica A 388 (2009) 4927.
[16] L.D. Pustylnikov, Trans. Moscow Math. Soc. 2 (1978) 1.
[17] A.L.P. Livorati, D.G. Ladeira, E.D. Leonel, Phys. Rev. E 78 (2008) 056205.
[18] F.A. de Souza, L.E.A. Simões, M.R. da Silva, E.D. Leonel, Math. Probl. Eng. (2009) Article ID 409857.
[19] E.D. Leonel, J. Phys. A: Math. Theor. 40 (2007) F1077.
[20] D.F. Tavares, E.D. Leonel, R.N. Costa Filho, Physica A 391 (2012) 5366.
[21] E.D. Leonel, M.R. da Silva, J. Phys. A 41 (2007) 015104.
[22] M.R. da Silva, D.R. da Costa, E.D. Leonel, J. Phys. A: Math. Theor. 45 (2012) 265101.
[23] U. Feudel, C. Grebogi, B.R. Hunt, J.A. Yorke, Phys. Rev. E 54 (1996) 71.
[24] U. Feudel, C. Grebogi, Chaos 7 (1997) 4.